Engineering of Light Electric Commercial Vehicle

R. Dorofeev[1], A. Tumasov[1], A. Sizov[1], A. Kocherov[1], A. Meshkov[1], D. Porubov[1]

[1]Nizhny Novgorod State Technical University named after R. E. Alekseev (Nizhny Novgorod,
 Russian Federation)

Abstract. The paper describes the process and results of the development of the light commercial electric vehicle. In order to ensure maximum energy efficiency of the developed vehicle the key parameters of the original electric motor. The article also presents the results of power electronic thermal calculation. For the mathematical model of the vehicle, the driving cycle parameters of the electric platform were determined in accordance with UNECE Regulations No 83, 84. The driving cycle was characterized by four successive urban and suburban cycles. The mathematical model also takes into account the time phases of the cycle, which include idling, vehicle idling, acceleration, constant speed movement, deceleration, etc. The model of the electric part of the vehicle was developed using MatLab-Simulink (SimPowerSystems library) in addition to the mechanical part of the electric car. The electric part included the asynchronous electric motor, the motor control system and the inverter. This model at the output allows to obtain such characteristics of the electric motor as currents, flows and voltages of the stator and rotor in a fixed and rotating coordinate systems, electromagnetic moment, angular speed of rotation of the motor shaft. The developed model allowed to calculate and evaluate the performance parameters of the electric vehicle. Technical solutions of the electric vehicle design were verified by conducting strength calculations. In conclusion, the results of field tests of a commercial electric vehicle are presented.

Keywords: electric vehicle, thermal analysis, electric drive, mathematical simulation, strength calculation

Разработка легкого коммерческого электромобиля

Р. Дорофеев[1], А. Тумасов[1], А. Сизов[1], А. Кочеров[1], А. Мешков[1], Д. Порубов[1]

[1]Нижегородский государственный технический университет имени Р. Е. Алексеева (Нижний Новгород,
 Российская Федерация)

Реферат. В статье описаны процесс и результаты создания легкого коммерческого электромобиля. С целью обеспечения максимальной энергоэффективности разрабатываемого транспортного средства определены основные параметры оригинального электродвигателя. Представлены результаты теплового расчета силовой электроники. Для математической модели транспортного средства определены параметры ездового цикла электрической платформы в соответствии с Правилами № 83, 84 ЕЭК ООН. Цикл движения характеризовался четырьмя последовательными циклами городского и пригородного режимов движения. Математическая модель также учитывает временные фазы цикла, которые включают холостой ход транспортного средства, ускорение, движение с постоянной скоростью, замедление и т. д. Модель электрической части транспортного средства разработана с использованием MatLab-Simulink (библиотека SimPowerSystems) в дополнение к механической части электромобиля. Электрическая часть включала асинхронный электродвигатель, систему управления двигателем и инвертор. Данная модель на выходе позволяет получить такие характеристики электродвигателя, как токи, поведение магнитного поля, напряжения статора и ротора в неподвижной и вращающейся системах координат, электромагнитный момент, угловая скорость вращения вала

Адрес для переписки
Дорофеев Роман
Нижегородский государственный технический университет
имени Р. Е. Алексеева
ул. Минина, 24,
603950, г. Нижний Новгород, Российская Федерация
Tel.: +7 9040 62-36-75
roman.dorofeev@nntu.ru

Address for correspondence
Dorofeev Roman
Nizhny Novgorod State Technical University
named after R. E. Alekseev
24 Minin str.,
603950, Nizhny Novgorod, Russian Federation
Tel.: +7 9040 62-36-75
roman.dorofeev@nntu.ru

Наука
итехника. Т. 19, № 1 (2020)
Science and Technique. V. 19, No 1 (2020)

63

двигателя. Разработанная модель позволила рассчитать и оценить параметры производительности электромобиля. Технические решения конструкции электромобиля были проверены на прочность путем расчетов. Представлены результаты полевых испытаний коммерческого электромобиля.

Ключевые слова: электрический автомобиль, температурный анализ, электрический привод, математическое моделирование, расчет прочности

Introduction

Road transport electrification is currently one of the main trends in the development of the global automotive industry (Along with the trends of increasing autonomy, shared use and inclusion in the information environment) [1]. Despite the fact that in 2015 the share of electric vehicles in the global fleet was insignificant – about 0.1 %, according to forecasts, this share will grow rapidly and will be about 10 % by 2030 and about 40 % by 2050 (in the estimates of the International Energy Agency only such types of electric vehicles as PHEV and BEV were taken into account) [2].

The main motivation for the spread of electric vehicles is associated with improved environmental performance and with a number of consumer characteristics: no noise motor, dynamic characteristics, etc. It is worth noting that the commercial transport has a significant impact on the environment because of constant operation with minimal downtime.

The key barriers to the spread of electric vehicles are:

– high cost of batteries/fuel cells;

– relatively low power reserve on a single charge;

– underdevelopment of infrastructure, first of all – charging stations.

Because of the barriers listed above, electric vehicle developers face an important and time-consuming task. It is to develop an energy-efficient electric drive system. This problem can be solved by an integrated approach to modeling the key components of the electric drive, the development of an adequate mathematical model of the electric car.

The object of the research

The GAZ Group is the leader on Russian market of commercial vehicles and holds about 70 % in the LCV category and 65 % in the LDT category [3]. The electrification was considered as the priority method to improve the environmental safety of this manufacturer products.

To implement the mentioned technologies, employees of the NNSTU, with the support of engineers from the Joint Engineering Center of the GAZ Group and specialists from PJSC GAZ, are working to create an electric platform for a light commercial vehicle (LCV) (Fig. 1). The chassis of the light commercial vehicle GAZelle NEXT was chosen as the object of research.

Fig. 1. The object of the research

Brief technical characteristics of the vehicle are presented in Tab. 1.

Table 1
Brief technical specifications of LCV GAZelle NEXT

Wheel arrangement	4×2
Drive type	Rear
Gross weight, kg	3500
Curb weight, kg * * *	2520
Load distribution of the vehicle total weight on the road through the tires, front wheels rear wheels, kg	1960 3745
Base, mm	3145/3745
Ground clearance (under the crankcase of the rear axle at full weight), mm	170
Minimum turning radius along the track of the outer front wheel, m	5.7/6.5
The maximum car speed on a horizontal section of a flat highway, km/h	130

64

Наука
и техника. Т. 19, № 1 (2020)
Science and Technique. V. 19, No 1 (2020)

Motor

The fundamental component of any electric drive is an electric motor. Thus, the energy efficiency of the electric vehicle as a whole will depend on how optimally the electric motor was selected. For this purpose, it was decided to develop an original electric motor for the developed electric platform.

As it is known, the mechanical characteristic of the motor has two distinct zones: a constant torque zone and a constant power zone. The ratio between the sizes of these zones significantly affects the choice of transmission ratio and dynamic characteristics of the vehicle [4]. The developed electric motor is designed to operate in two modes with different values of mechanical torque and duration. By preliminary traction calculation target mechanical characteristics of the electric motor were determined (Tab. 2, Fig. 2).

Table 2

Motor characteristics

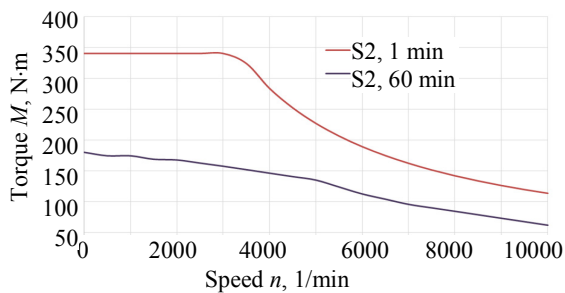| Characteristic	Value
Motor type	Asynchronous
Number of phases	3
Rated voltage, V	400
Maximum revolutions, rpm	10000
Maximum power, kW	47
Cooling system	Liquid type
The type of construction in accordance with IEC 600034-7	IM B5
Maximum height of use above sea level according to IEC 600034-1, m	Not more than 2500 without power reduction
Insulation temperature class according to IEC 600034-1	H
Protection degree in accordance with IEC 600034-5	IP65
Radial shaft run-out class according to DIN 42955	N
Noise level according to DIN EN ISO 1680	75dB+3dB
The level of vibration according to IEC 600034-14	Level A
Ambient temperature	From –40 °C to +70 °C

Fig. 2. Mechanical characteristics of the electric motor

At the initial stage of the motor design the optimal configuration of the rotor and stator slots were determined (Fig. 3).
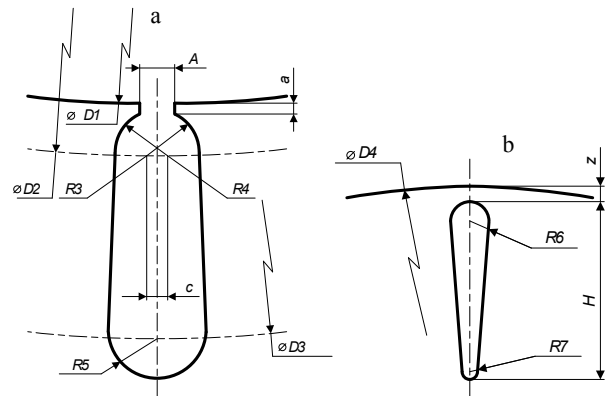

Fig. 3. Shape of stator (a) and rotor (b) slots

The stator has semi-open for laying the winding. The stator is made of electrotechnical steel plates with a thickness of 0.27 mm. Rotor is made of electrical steel plates the same as the stator. The rotor has closed oblong shape slots for the placement of short-circuited winding roads. The short-circuited winding is performed by pouring the rotor set with aluminum under pressure. Structurally, the winding is made of soft multi-strand Litz wire and placed in the stator slots. A winding is a group of coils connected in a star pattern, herewith such a winding cannot be considered as containing two parallel coils in each phase, since the middle points of the coil groups are not combined.

During the design of the electric motor, several prototypes were created to test the assumptions inherent in the calculation models [5, 6].

In the process of the electric motor model preparing the boundary conditions were given. The outer contour of the magnetic system is specified as a first class boundary condition, magnetic potential $\varnothing = 0$. The rest of the boundary conditions were determined automatically by the numerical simulation system in accordance with the materials and current-carrying areas. After setting the boundary conditions, a finite elements grid was constructed. Triangles were used as grid elements (Fig. 4).

During the calculation process, the solver automatically rebuilt the grid to achieve the specified accuracy of the solution. In the process of solving, 6 grid rearrangements were made. As a result, the number of grid elements was increased from 14.734 to 56.574. The error in determining the magnetic field energy at the last iteration

■Наука
итехника. Т. 19, № 1 (2020)
Science and Technique. V. 19, No 1 (2020)

65

of the solution was 0.009 %. In the process of solving the distribution of the magnetic field in the motor parts material was obtained. Fig. 5 shows the distribution of magnetic induction in the motor parts. The maximum value of the magnetic field induction was 1.7105 T.

As a result of modeling, the greatest electromagnetic losses in absolute value caused by an alternating electromagnetic field were determined. Losses in absolute value are the sum of losses that are different in nature:

– losses in the winding wires determined by the Joule – Lenz law;

– hysteresis losses;

– eddy current losses.

Maximum losses were 6391 W at speeds from 2100 rpm to 3900 rpm.

Despite the total loss of almost 6.4 kW, the motor has an efficiency of 95 % in this range (Fig. 6). The efficiency is reduced in the zone of lowest speed and in the constant power end zone after 4000 rpm. In the high revs from 6000 rpm the motor torque and its efficiency are significantly reduced. Operation in this speed range is not recommended. The current distribution has a maximum of 219 A at the end of the constant torque zone. The maximum power of the electric motor was 81 kW (Fig. 6).
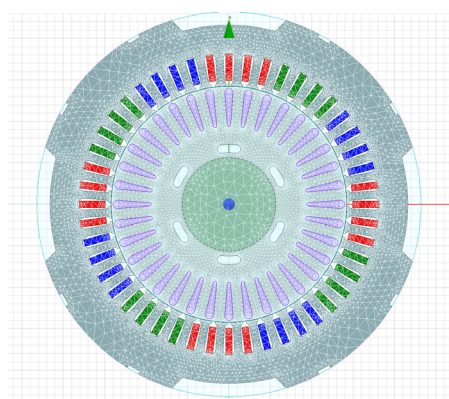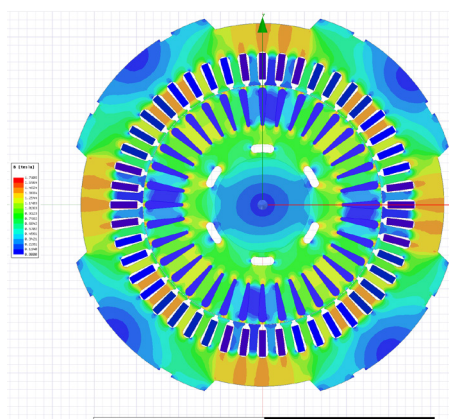

Fig. 4. Finite elements grid

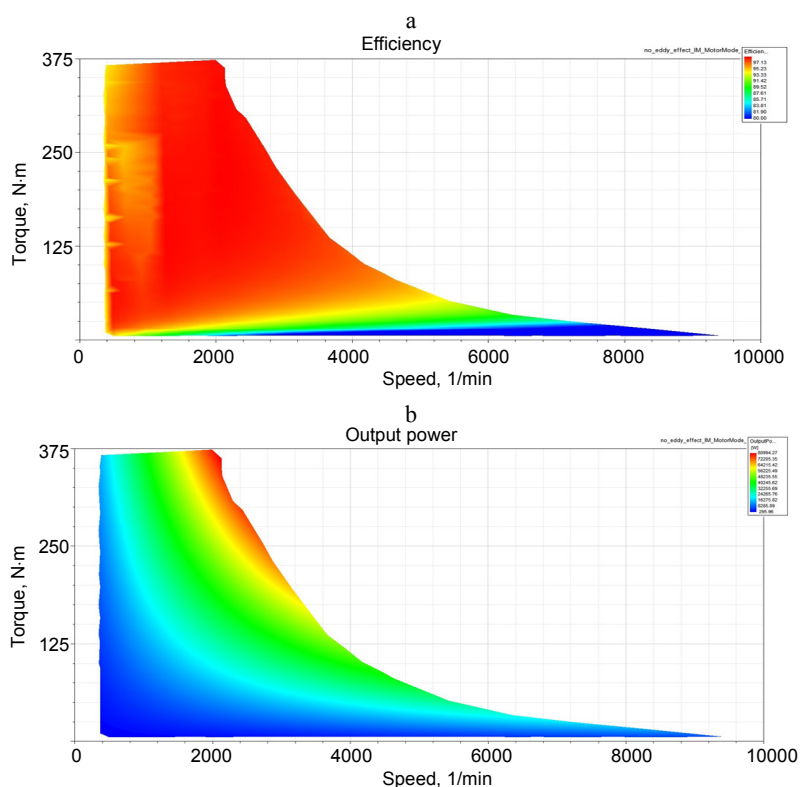*Fig. 5.* Magnetic induction distribution in motor parts

Fig. 6. Efficiency (a) and power (b) distribution

66

Наука
итехника. Т. 19, № 1 (2020)
Science and Technique. V. 19, No 1 (2020)

Thermal modeling

The objects of thermal modeling were the electric motor and the battery subpack.

The information about the heat release in the motor parts was transmitted from the results of the electromagnetic calculation obtained earlier. The boundary conditions for the thermal calculation of the electric motor were adopted as follows: the ambient temperature of 55 °C and the heat transfer coefficient of 5 W/(m²·deg). The assumed value of the heat transfer coefficient corresponds to natural convection in cramped conditions in the absence of external airflow. These conditions are obviously worse than the operating (maximum operating temperature of the motor is 40 °C). The geometric model of the electric motor liquid circuit and the results of thermal calculation are presented in Fig. 7.
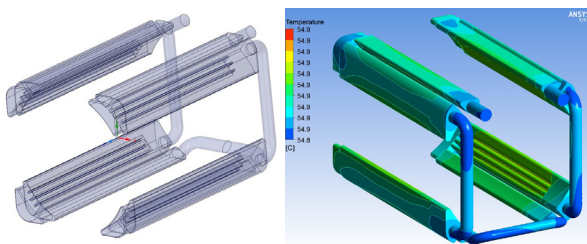

Fig. 7. Geometric model of the motor liquid circuit
and the results of thermal calculation

Table 3

Calculated thermal-hydraulic parameters

Parameter	Unit
Maximum stator temperature, °C	55
Maximum temperature of stator windings, °C	55
Maximum rotor temperature, °C	55
The maximum temperature of the rotor closed-loop winding, °C	55
Maximum coolant temperature, °C	55
Coolant temperature at the outlet of the cooling channels, °C	55
Pressure drop between inlet and outlet of cooling channels, °C	10000

To calculate the thermal state of the battery subpack elements, it is necessary to specify the heat sources and heat transfer conditions between the subpack structural elements. The main sources of heat are battery cells, with the heat release of 38830 W/m³. On the outer surfaces of the battery subpack elements, the convective heat exchange condition similar to that of an electric motor was set. The geometric model of the battery subpack and the thermal calculation results are presented in Fig. 8.
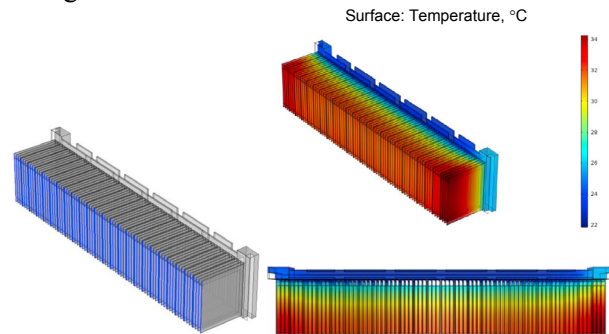

Fig. 8. Geometric model of the battery subpack
and thermal calculation results

In calculation process the temperature distribution in the battery subpack elements (Tab. 4), the coolant temperature at the outlet of the cooling system channel, the coolant pressure drop between the inlet and outlet of the cooling system channels, as well as general information about the nature of the coolant flow in the cooling channels were obtained.

Table 4

Calculated thermo-hydraulic parameters

Parameter	Unit
Pressure drop between inlet and outlet of cooling channels, Pa	11125
Coolant temperature at the outlet of the cooling channels, °C	23.9
Maximum battery cell temperature, °C	33.2
Average battery cell temperature, °C	28.4

The maximum temperature of the cell was 33.2 °C. This value was higher than the upper value of the battery cell operating temperature equal to 30 °C. These temperature values are in an area that is poorly cooled by the radiator coolant since the radiator channel does not cover the entire heat exchange surface with L-shaped radiators. It is recommended to either reduce the number of cells in the radiator, or extend the flow of the radiator in such a way as to provide a more uniform cooling of the battery cells.

Mathematical modeling

The process of mathematical modeling of the electric platform was divided into three technical

■ Наука
итехника. Т. 19, № 1 (2020)
Science and Technique. V. 19, No 1 (2020)

67

parts: mechanical, electrical and motor control parts. For the mechanical part, a model has been developed to calculate the necessary amount of power required to drive at a given speed, in which the resulting power is due to the sum of all the resistance forces to the electrical platform movement, the same approach will be applied to the evaluation of the recovery energy returned to the battery by braking the vehicle.

In the electrical part, the general circuitry of the electric vehicle including its main parts is considered: an asynchronous motor, an inverter and a battery. It will make it possible to estimate the total run-out of the vehicle in a given driving mode. This unit has a direct connection with the mechanical part. Each part will be assembled separately according to the automobile mathematical equations theory and the theory of electric machines. All created subsystems interacted with each other in the process of modeling the car movement-braking. The calculation was performed in one-dimensional design environment by means of Matlab Simulink block package.

To assess the possibility of the car movement, it is necessary to analyze the scheme shown in Fig. 9, which shows the main forces involved in the car movement. These forces include the driving force realized on the driving wheels in the form of traction torque and forces that create resistance to movement [7].
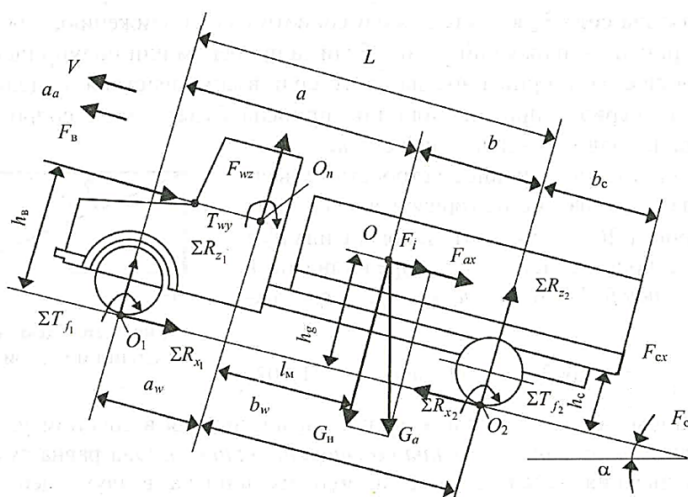

Fig. 9. Forces and torques acting on the car in the general case of motion

A general equation characterizing the rectilinear motion of the car with a trailer in general was written down

$$F_{to} - F_\psi - F_b - F_a = 0,$$

where F_{to} – traction force on the driving wheel; F_ψ – road resistance force: the wheel rolling resistance force and of resistance force to rise; F_b – resistance force of the incoming air flow during the car movement; F_a – inertial force or resistance force to translational motion.

Traction force on the car driving wheels

$$F_{to} = \frac{T_e u_{tr} \eta_{tr}}{r_d} - \frac{(\gamma_e T_e + J_e)\varepsilon_e u_{tr}\eta_{tr}}{r_d},$$

where T_e – engine crankshaft torque, N·m; u_{tr} – transmission ratio; η_{tr} – vehicle transmission efficiency; r_d – wheel free radius, m.

Road resistance force

$$F_\psi = f_{aw} G_a \cos\alpha \pm G_a \sin\alpha,$$

where f_{aw} – road resistance coefficient; G_a – vehicle force weight, N; a – lifting gradient angle, deg.

Air resistance force

$$F_b = 0.5 c_x \rho_b A_b v_w^2,$$

where c_x – vehicle drag coefficient; ρ_b – air density; A_b – midsection area, m^2; v_w – vehicle speed, m/s.

Inertial force

$$F_a = \delta m_a a_a,$$

where m_a – vehicle weight, kg; a_a – vehicle acceleration, m/s^2; δ – rotating masses coefficient

$$\delta = 1 + \sigma_1 u_k^2 u_d^2 + \sigma_2;$$

u_k – transmission ratio; u_d – gear ratio of the additional gearbox;

$$\sigma_1 = \frac{(\gamma_e T_e + J_e)u_0^2 \eta_{tr}}{m_a r_d r_k};$$

$$\sigma_2 = \frac{\sum J_k}{m_a r_d r_k}.$$

For most vehicles, values are taken in the following ranges $\sigma_1 = 0.03$–0.05; $\sigma_2 = 0.04$–0.06 [7].

To obtain an adequate mathematical model of the electric platform, it is necessary to choose the

most typical picture of the speed changing process and acceleration of the vehicle in question, taking into account the movement regional specifics in different conditions. This process must contain both the urban movement cycle and the suburban driving cycle. Such an evaluation regime can be a test cycle according to GOST R EN 1986-1–2011 [8] (analogue of the European driving cycle – NEDC (New European Driving Cycle) used to assess the toxicity of vehicles [9]).

At the same time, the urban cycle itself is characterized by the duration of 195 s and includes the following time phases (Fig. 10):

– idling for 60 s;
– vehicle idling for 9 s;
– gear change time, lasting 9 s;
– acceleration, lasting 36 s;
– driving time at a constant speed of 57 s;
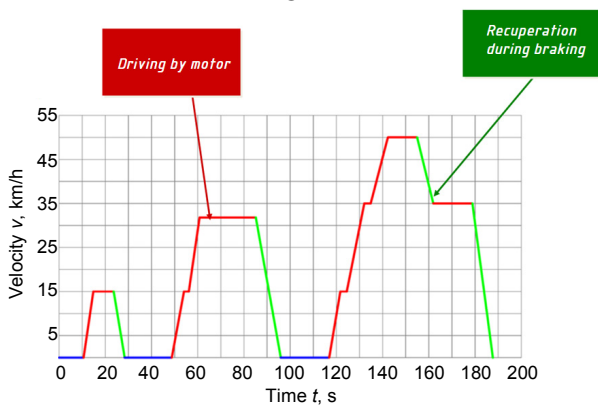– deceleration, lasting 25 s.

Fig. 10. Diagram of a simple urban cycle

In this cycle, the vehicle must travel with four main speed limits: 15 km/h (4.17 m/s), 32 km/h (8.9 m/s), 35 km/h (9.72 m/s) and 50 km/h (13.9 m/s); five main positive acceleration limits: 1.04 m/s^2, 0.69 m/s^2, 0.79 m/s^2, 0.51 m/s^2, 0.46 m/s^2; and the following main negative acceleration limits: –0.83 m/s^2, –0.81 m/s^2, –0.52 m/s^2, –0.97 m/s^2.

Fig. 11 shows the speed dependence of the suburban cycle. For this cycle, the average speed is within 62.60 km/h and the distance covered is 6956 m.

The country cycle is characterized by duration of 400 s and includes the following time phases:

– stop for 40 s;
– acceleration, lasting 109 s;
– constant speed driving time 209 s;
– deceleration, lasting 42 s.

In this cycle, the vehicle must travel with four main speed limits: 50 km/h (13.9 m/s), 70 km/h (19.4 m/s), 100 km/h (27.8 m/s) and 120 km/h (33.3 m/s); six main positive acceleration limits: 0.69 m/s^2, 0.51 m/s^2, 0.42 m/s^2, 0.43 m/s^2, 0.24 m/s^2, 0.28 m/s^2; and the following main negative acceleration limits: –0.69 m/s^2, –1.04 m/s^2, –1.39 m/s^2.

Fig. 12 shows the assembled circuit of the electric platform mechanical part calculating the consumed-renewable power for the selected driving cycle. In this case, the model takes into account all the technical features of the designed electric platform: transmission ratios and its efficiency. Also, the calculation model includes parameters such as the gross mass involved in the calculation of the resistance forces to movement and the Midsection coefficient, which characterizes the car cross-sectional area.
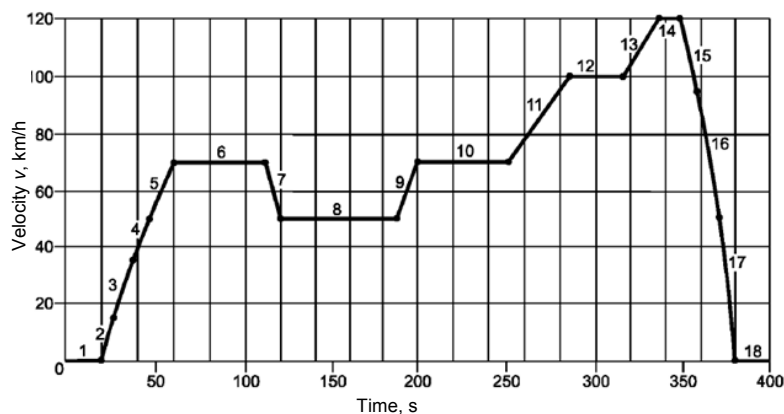

Fig. 11. Suburban cycle diagram

Наука
итехника. Т. 19, № 1 (2020)
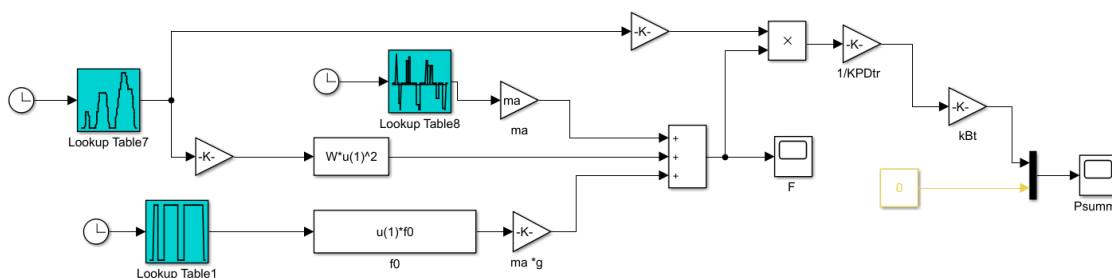Science and Technique. V. 19, No 1 (2020)

69

Fig. 12. Mixed cycle diagram for a vehicle with a gross weight of up to 3.5 t

For the convenience and simplicity of modeling the electrical part of the electric platform, blocks of the SimPowerSystems library containing all the necessary electrical part components of the designed electrically powered vehicle were used. This approach can reduce the design time of complex electrical parts, increase the computational model performance, simplifying the calculation and reducing the calculation time. Thus at the design stage and the effectiveness evaluation of the developed electrical platform it can significantly reduce the time to run test models.

To model an asynchronous machine with a squirrel-cage rotor, the standard asynchronous machine unit is used. It can be applied in two modes: as an electric motor and a generator [10].

To create a model of an inverter that converts DC to AC, a "universal bridge" block from the standard library SimPowerSystems Simulink application is used. This unit allows to create a number of semiconductor devices (diodes, thyristors, ideal keys, as well as fully controlled thyristors, IGBT and MOSFET transistors shunted by reverse diodes) [10].

The battery was simulated using a standard battery pack, which can also be found among SimPowerSystems applications in a Simulink environment. This model contains the main types of self-discharging batteries that are currently the most common in technical equipment. This unit contains four types of batteries with different physical and chemical properties, taking into account different parameters, from the initial charge of the battery to the temperature modes of charge and self-discharges. This device is suitable for quick efficiency evaluation of the power supply and allows evaluating the various advantages of each of the presented battery types.

Fig. 13 shows the equivalent scheme of the battery pack under consideration.

Fig. 14 shows the assembled electrical part circuit of the electrical platform. This scheme consists of a standard asynchronous motor unit, which is fed to the design torque obtained in the mechanical part of the mathematical model. The induction motor is powered by a three-phase voltage generated in the inverter. The signal for the inverter is a control unit that regulates the angular velocity calculated in the model mechanical part.

There is a battery in the circuit diagram of the electric part unit. In this case, a Nickel-metal hydride battery with a voltage of 400 V and a capacity of 140 Ah is shown.
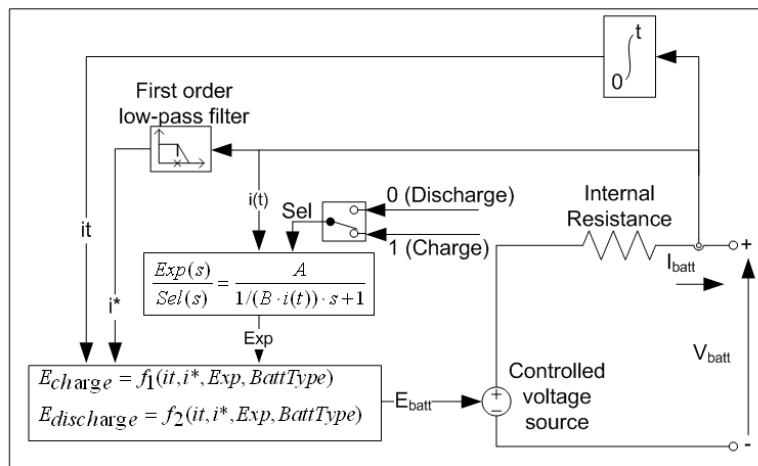

Fig. 13. Battery equivalent circuit

70

■Наука
и技ника. Т. 19, № 1 (2020)
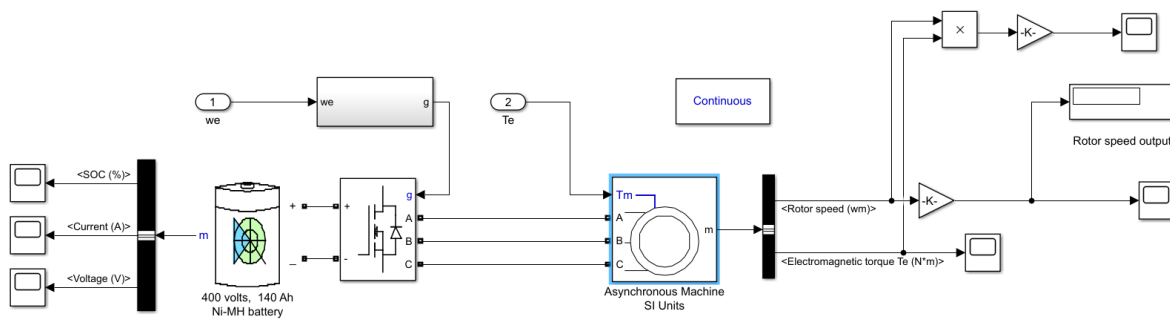Science and Technique. V. 19, No 1 (2020)

Fig. 14. Electrical part of electric platform with engine speed control unit

By connecting the mechanical and electrical parts of the electrical platform a general mathematical model of the developed vehicle, shown in Fig. 15, is obtained.

The developed model will allow calculating and evaluating the efficiency parameters of the traction electric drive of electric platforms.

To assess the effectiveness of the electric platform, a review of batteries in the modern market was conducted, since, as previously noted, it is the power sources that are one of the main elements of the electric vehicle traction system. This element directly determines both the car traction and speed characteristics, and its full power reserve.

Based on the given technical parameters of the cells, several possible power sources of the electric platform for the calculating case are formed. The most common voltage in electric commercial vehicles is 400 V. Blocks consisting of the basic power sources (cells) connected in series to each other and batteries are formed and summarized in Tab. 5.

To analyze the energy efficiency, 4 models of the battery are formed. For each of the considered battery the desired amount of energy required to move a given speed, according to the selected mode of the elementary urban cycle with duration of 195 s is calculated according to GOST R EN 1986–2011. The calculation determined the values of the re-

quired energy for movement in the elementary cycle. On the basis of the designed electrical platform where was a mathematical model of the battery discharge the following predicted values of the reserve shown in Tab. 5 were obtained. It is worth noting that in these calculation models were not taken into account additional power sources, such as air conditioning, external and internal lighting, etc., which can reduce the total mileage.

Table 5

Expected power reserve of the electric platform

Battery	Battery specifications	Quantity on the prototype	Expected cruising range, km
1	$V = 400$ V $C = 36$ Ah $m = 207$ kg	2	108
2	$V = 400$ V $C = 40$ Ah $m = 200$ kg	2	120
3	$V = 400$ V $C = 35$ Ah $m = 150$ kg	2	105
4	$V = 400$ V $C = 40$ Ah $m = 200$ kg	2	120

Based on the above, it is recommended to use battery No 2 as a power source for the electric platform as an effective option among the considered batteries.
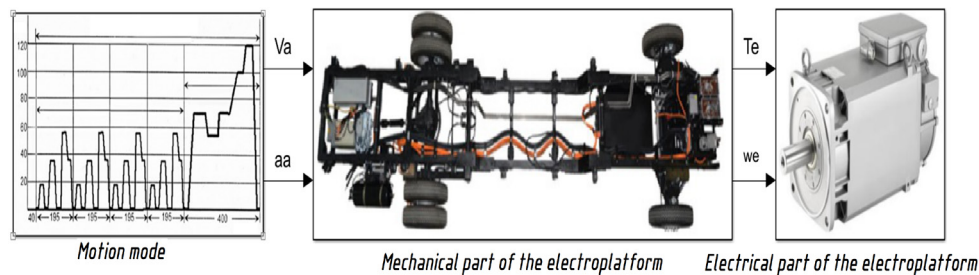

Fig. 15. Electric platform model

Наука
итехника. Т. 19, № 1 (2020)
Science and Technique. V. 19, No 1 (2020)

71

Strength calculation

At the design stage of the electroplaters light commercial vehicle it was required to analyze the comparative stiffness of the middle suspension battery for basic configuration and for the variant with the welded corners reinforcement inside and out.

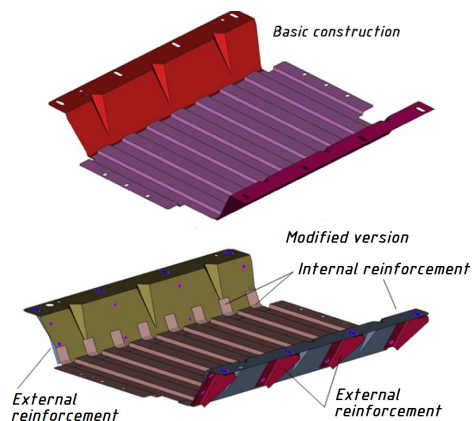Fig. 16 shows the design diagram for the two variants of the electric vehicle battery suspension.

Fig. 16. Structural diagrams of battery suspension options

Four design options were considered:
– basic configuration;
– option where interior and exterior corners are added on both sides;
– the same, but the outer corners of the "flat" side are missing;
– option only with outer corners on both sides.

To determine the stiffness in the transverse direction to the structure forces were applied (Fig. 17):

1000 N at the lower midpoint (point *A*);

300 N at the upper midpoint (point *B*).

In addition, the structure was loaded with its own weight.

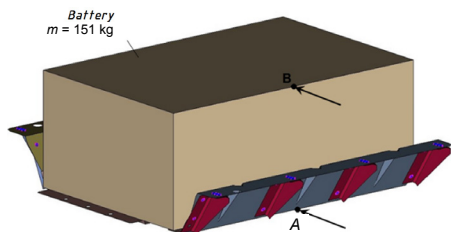The calculation results are summarized in Tab. 6.

Fig. 17. Force application diagram

According to the results of the calculations, with the use of full reinforcement (inside and outside on both sides), the transverse rigidity of the battery suspension structure of the electric vehicle increases by about 8 times. At the same time the eigen frequency of the structure increases in the transverse direction.

Table 6

Calculation results

	1st eigen frequency, Hz	Movement with 1 kN force applied at the bottom point, mm	Movement with 300 N force applied at the upper point, mm
Basic version	6.47	1.42	1.56
The option with the outer corners of one side + internal corners	17.4	0.29 (490 %)[*]	0.34 (459 %)[*]
The option with the outer corners on both sides + inner corners	22.9	0.16 (888 %)[*]	0.20 (780 %)[*]
Option with outer corners on both sides, but without inner corners	20.1	0.23 (617 %)[*]	0.29 (538 %)[*]
[*] In parentheses there is percentage increase in stiffness compared to the base case.			

Additionally, the strength calculation of the electric vehicle frame was carried out.

Fig. 18 shows a structural diagram for the calculation of the light commercial electroplater frame.
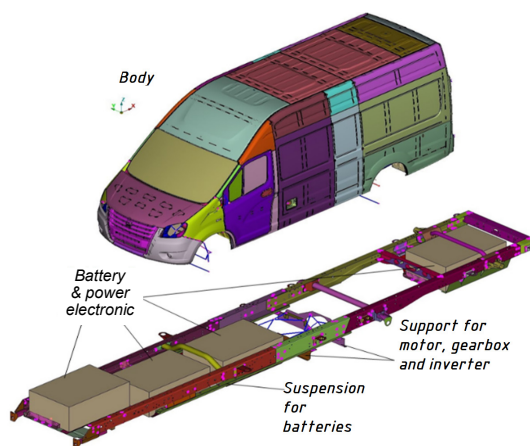

Fig. 18. Structural diagram of the frame calculation

The nominal weight of the loaded electric platform was assumed to be equal to 3.5 t. The cargo weight (1.2 t) was evenly distributed over 3 euro pallets 1200×800 mm, fixed to the body floor.

In the context of work 2 design cases were discussed: triple vertical overload and front wheel hanging.

In the case of a triple vertical overload, a triple gravitational load was applied to the model in the

72

Наука
итехника. Т. 19, № 1 (2020)
Science and Technique. V. 19, No 1 (2020)

vertical direction with acceleration equal to 3g =
= 3 · 9810 = 29430 mm/s².

In the case of the front wheel hanging the torque was applied to the front axle midpoint

$$M_x = \frac{Gbc}{2(a+b)},$$

where $G = mg$ – gross vehicle weight; m – total weight, t; $c = 1750.2$ mm – front chassis base (distance between the wheels); a, b – see the diagram in Fig. 19.

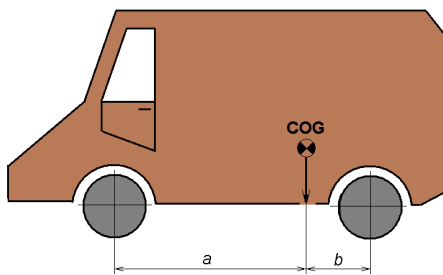Thus $a = 2220.06$ mm; $b = 1418.64$ mm; $m = 4{,}05$ t; $M_x = 1.354 \cdot 10^7$ N·mm.

Fig. 19. Mass center position of the model relative to the axes

Calculation results

1. Case of triple vertical overload

The calculation results are shown in Fig. 20. The maximum equivalent voltages (564 MPa) will be in the rear pallet corrugation zone.
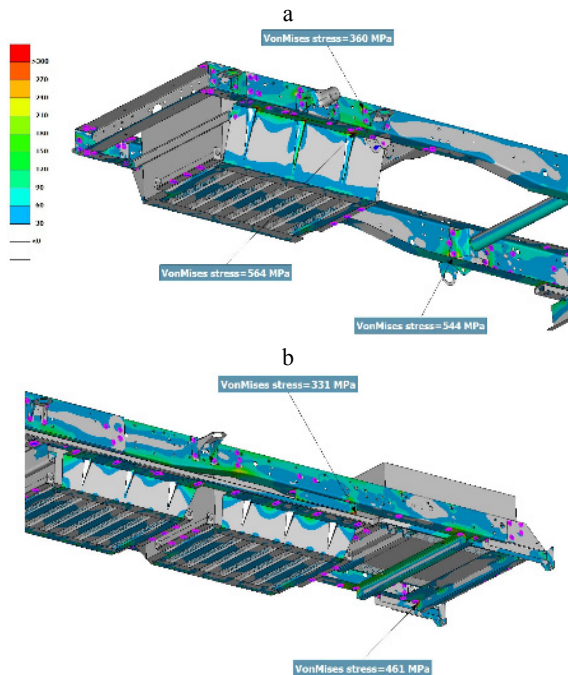

Fig. 20. Equivalent stresses according to Mises, MPa, triple vertical acceleration: a – rear part; b – front part

2. Front wheel hanging case

The calculation results are shown in Fig. 21. The maximum equivalent stresses (450 MPa) will be in the area of the junction of the front crossbar under the battery with the spar.
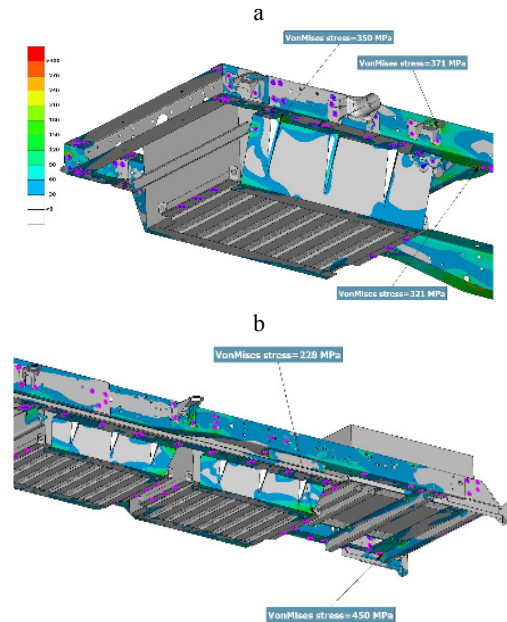

Fig. 21. Equivalent stresses according to Mises, MPa, front wheel hanging case: a – rear part; b – front part

Running tests

The purpose of the tests was: to set the power reserve for the developed electric light comercial vehicle, to fix the mileage of the vehicle as the charge level of the traction battery decreases.

The GAZ Group's motor range in the Berezovaya Poima settlement was used as the test site. The test conditions correspond to the normal climatic conditions specified in paragraph 5.2 [11] (T5-temperate climate). The actual ambient temperature was 27 °C.

The vehicle was weighed in running order, then the vehicle was loaded to the full weight of 3.5 (Fig. 22).

The vehicle was installed on a flat horizontal surface. The CAN adapter PCAN-USB X6 CAN-FD (hereinafter referred to as the CAN Adapter) was connected to the vehicle's on-board network, the Racelogic VBOX 3i RTK multifunction speed meter kit was installed and connected.

The following parameters were recorded during the test:

– the coordinates of the vehicle location (speed);

Наука
итехника. Т. 19, № 1 (2020)
Science and Technique. V. 19, No 1 (2020)

73

– battery charge level;

– fixing the maximum and average speed on the track;

– vehicle mileage until the battery is fully discharged;

– the voltage level in the traction battery;

– current consumption and current recovery;

– time.

Fig. 22. Vehicle weighing in running order

The first type of the test is traffic simulation in the city.

The tests were carried out at the vehicle test site (50 % of the time) and on straightforward sections of the asphalt road (Fig. 23). Maximum speed 50 km/h (±5), the average speed for the entire run was at least 22 km/h.

In the process and according to the test results, the following values were recorded:

– average and maximum speed on the track;

– mileage at battery discharge from 90 to 60 %;

– mileage reach time 50 km.

At the beginning of the tests, the charge level of the traction battery was 92 %, and the voltage on the battery was 379 V.

To determine the indicators, the test driver was driving at a speed of not less than 22 km/h and not exceeding 50 km/h. According to the test results, the average speed on the track was 24 km/h, the maximum – 55 km/h. Results are presented in Tab. 7.

The second type of test-driving cycle.

The vehicle was tested in cycles. One cycle includes: acceleration to 10 km/h, movement at a speed of 10 km/h for 1 min, stop. Repetition of

acceleration and movement with speeds multiple of 10 up to 60 km/h. According to the test results, the following parameters were determined:

– the total number of cycles during the test before the battery is fully discharged;

– maximum speed during tests;

– vehicle mileage before full battery discharge (10 %);

– vehicle mileage at a charge level of 90 to 10 %, in increments of 10 %.

Fig. 23. Test location

Table 7

Vehicle movement parameters. The first type of test

Battery charge, %	Voltage on battery, V	Mileage, m
90	394	2495
80	385	16417
70	371	32894
60	371	48722

At the beginning of the tests, the charge level of the traction battery was 98 %, the voltage on the battery was 397 V.

To determine the total number of cycles during the test, the test driver accelerated the vehicle to a speed of 10 km/h and moved at this speed for 1 min. Then it stopped completely. The acceleration and the movement were repeated at speeds that are multiples of 10 to 60 km/h. The total number of cycles during the test until the battery discharge to 10 % was 22 cycle. This test was carried out 1 time. The vehicle was accelerated to a maximum speed. The maximum speed of the vehicle during the tests was 102 km/h.

74

Наука
иТехника. Т. 19, № 1 (2020)
Science and Technique. V. 19, No 1 (2020)

According to the data presented in Tab. 8, the vehicle mileage was 112.9 km at battery discharge from 98 % to 10 %.

Table 8

**Vehicle movement parameters.
The second type of test**

Battery charge, %	Voltage on battery, V	Mileage, m
90	385	11539
80	371	25921
70	368	40673
60	353	55270
50	349	67862
40	334	78705
30	331	93314
20	323	102090
10	331	112977

CONCLUSION

According to the results of the tests, it can be concluded that the battery charge of the developed electric vehicle, with a total weight of 3500 kg, is enough to overcome the distance of more than 100 km, at a temperature of 20 degrees and above. The discrepancy between the values of the mileage obtained experimentally and theoretically was less than 6 %. Thus, we can talk about the adequacy of the developed mathematical model of the electric vehicle. The results of this work will be a good starting point for the development of energy-efficient electric commercial vehicles.

REFERENCES

1. Knupfer S. M., Hensley R., Hertzke P., Schaufuss P. (2017) *Electrifying Insights: How Automakers Can Drive Electrified Vehicle Sales and Profitability.* Available at: https://www.mckinsey.com/industries/automotive-and-assembly/our-insights/electrifying-insights-how-automakers-can-drive-electrified-vehicle-sales-and-profitability.
2. International Energy Agency (2016) *Global EV Outlook 2016 Beyond One Million Electric Cars.* https://doi.org/10.1787/9789264279469-en.
3. *Commercial Vehicles.* Available at: https://rim3.ru/comauto/news/perspektivy-gruppy-gaz/ (Accessed 30 May 2018) (in Russian).
4. Vol'dek A. I., Popov V. V. (2010) *Electrical Machines. AC Machines.* St. Petersburg, Piter Publ. 356 (in Russian).
5. Hameyer K., Belmans R. (1999) *Numerical Modeling and Design of Electrical Machines and Devices.* Boston, WITpress, 340.
6. Bianchi N. (2005) *Machine Analysis Using Finite Elements.* Boca Raton CRCpress, 290. https://doi.org/10.1201/9781315219295.
7. Kravets V. N., Selifonov V. V. (2011) *The Theory of a Car.* Moscow, OOO "Greenlight +", 884 (in Russian).
8. GOST 1986-1–2011 *Electrically Propelled Road Vehicles. Measurement of Energy Performances. Part 1. Pure Electric Vehicles.* Moscow, Standartinform Publ. 2012, 19 (in Russian).
9. UNECE No 83, 84 *Uniform Provisions Concerning the Approval of Vehicles with Regard to the Emission of Pollutants According to Engine Fuel Requirements.* Available at: https://www.unece.org/fileadmin/DAM/trans/main/wp29/wp29regs/R083r5e.pdf.
10. Chernyh I. V. (2008) *Modeling of Electrical Devices in MatLab, SimPowerSystems i Simulink.* Moscow, DMK Press Publ. 288 (in Russian).
11. GOST R 15150–69 *Machines, Instruments and Other Industrial Products. Modifications for Different Climatic Regions. Categories, Operating, Storage and Transportation Conditions as to Environment Climatic Aspects Influence.* Moscow, Standartinform Publ. 2006, 59 (in Russian).

Наука
итехника. Т. 19, № 1 (2020)
Science and Technique. V. 19, No 1 (2020)

75